

Fabrication and Application of an Okra-Derived Sorbent for Efficient Removal of Acetaminophen Micropollutants from Aqueous Media

Tuba ERSEN DUDU^{a,b,*}, Duygu ALPASLAN^{a,b}

^a Department of Chemical Engineering, Institute of Natural and Applied Science, Van Yuzuncu Yil University, Van, 65080, Turkey; ^b Department of Mining Engineering, Faculty of Engineering, Van Yuzuncu Yil University, Van, 65080, Turkey

Abstract Pharmaceutical micropollutants, such as acetaminophen, pose increasing environmental concerns due to their persistence in aquatic systems. In this study, a novel bio-based sorbent was synthesized from agricultural okra waste via redox polymerization in the presence of nickel ions (Ni). The resulting p(Okra)/Ni composite particles were thoroughly characterized through structural and morphological analyses, confirming their successful formation. Batch sorption experiments were performed under different pH, temperature, sorbent dosage, and initial acetaminophen concentration conditions. Among the synthesized materials, p(Okra)/Ni₁ and p(Okra)/Ni₃ showed the highest sorption performance, with maximum acetaminophen sorption capacities of 507.6 mg/g and 452.2 mg/g, respectively. The highest sorption capacities achieved at optimum sorbent dosage were 592.1 mg/g for p(Okra)/Ni₁ and 566.1 mg/g for p(Okra)/Ni₃. Sorption was strongly influenced by pH and temperature, with optimum performance observed near neutral pH. Equilibrium data were best described by the Langmuir isotherm model ($R^2 > 0.99$), indicating monolayer sorption on homogeneous active sites. BET analysis revealed surface areas between 83.7 and 88.4 m²/g, while pore volume and pore diameter increased with increasing Ni content. Overall, the developed p(Okra)/Ni sorbents demonstrated high efficiency for acetaminophen removal and offer a sustainable approach for converting agricultural waste into value-added materials for wastewater treatment.

Keywords: Acetaminophen, biopolymer, sorption mechanism, sustainable materials, water treatment.

Introduction

With the rise in global population and industrial development, the availability and quality of water resources are increasingly threatened by scarcity and pollution. Recent studies have identified pharmaceutical-derived micropollutants as significant contributors to environmental and aquatic contamination, with harmful effects on ecosystems [1-5]. Many of these micropollutants resist biological degradation, and conventional wastewater treatment plants are often ineffective at their complete removal. As a result, these pollutants may enter the environment untreated, or previously adsorbed compounds in treatment sludge and soils may desorb, subsequently contaminating surface and groundwater. Pharmaceuticals that are insufficiently treated and discharged into rivers, lakes, seas, and aquifers pose serious risks to both environmental and human health [6-9].

Current biological treatment methods are inadequate for removing active pharmaceutical ingredients that threaten both human and ecological well-being. To address this limitation, advanced treatment technologies must be integrated with biological methods. Techniques such as ozonation, ultrafiltration-reverse osmosis, coagulation-flocculation, filtration, physicochemical processes, and adsorption/absorption (sorption) are being investigated as potentially effective complementary approaches [10–13]. Among these, sorption stands out due to its high efficiency, broad applicability,

***For correspondence:**

tubaersendudu@yyu.edu.tr

Received: 04 December 2025

Accepted: 15 June 2026

©Copyright Dudu. This article is distributed under the terms of the [Creative Commons Attribution License](#), which permits unrestricted use and redistribution provided that the original author and source are credited.

ease of implementation, low cost, and absence of secondary pollution, making it particularly suitable for the removal of micropollutants [12,14]. Various materials, including natural and synthetic polymers, activated carbon, silica gel, graphene oxide, zeolites, and clays, have been studied as potential sorbents [15–16]. Notably, recent studies have highlighted the potential of biomass-derived carbon materials, which offer large surface areas and tunable surface functionalities for effective sorption [17]. In this context, sustainable, biomass-based materials are gaining increasing attention due to their environmental compatibility and customizable physicochemical properties [18-19].

Recently, there has been growing interest in the use of natural polymers from renewable sources in sorption applications. Bio-based materials are biodegradable, abundantly available, non-toxic, cost-effective, and renewable, making them excellent candidates for super adsorbents due to their polysaccharide, protein, lignin, and fibrous structures. Bio-based adsorbents derived from polysaccharides and lignocellulosic biomass have demonstrated considerable potential in this field [20]. Okra, a low-cost and renewable source of biopolymers, has shown promise for removing environmental pollutants from aqueous media due to its biodegradability and non-toxic nature [21–22]. Beyond its nutritional value, okra has been investigated for use in medical, food, and industrial applications, including the development of polymeric sorbent particles [23]. It contains heteropolysaccharides composed of rhamnose, galacturonic acid, galactose, glucose, and glucuronic acid, which form a viscous, mucilaginous solution when extracted with water. These polysaccharides are currently being studied for both pharmaceutical and environmental applications [24-28].

In recent years, the widespread consumption of acetaminophen, especially during the COVID-19 pandemic, has contributed to its global presence in aquatic environments. Recognizing the ecological risks posed by such pollutants, this study aims to synthesize okra/metal-based polymeric particles for the first time, using a redox polymerization technique in an emulsion system with okra extract obtained from agro-waste. Nickel ions were incorporated to introduce the metal component, and the resulting particles were specifically designed to remove acetaminophen from contaminated water. The structural and physicochemical characteristics of the synthesized particles were investigated using scanning electron microscopy (SEM), Fourier-transform infrared spectroscopy (FTIR), Brunauer–Emmett–Teller (BET) surface area analysis, thermogravimetric analysis (TGA), dynamic light scattering (DLS), and zeta potential measurements. Sorption experiments were conducted under varying acetaminophen concentrations, pH levels, temperatures, and particle dosages to evaluate sorption efficiency. Additionally, sorption isotherms and thermodynamic parameters were modeled and analyzed to better understand the sorption mechanism. This study presents a promising and sustainable approach for the treatment of pharmaceutical-contaminated water, contributing to broader efforts in the development of green and effective sorbents [29].

Materials and Methods

Materials

The chemicals used in this study were ethanol (96%, C₂H₅OH, Sigma-Aldrich), ethylene glycol dimethacrylate (EGDMA, 99%, as a cross-linker, Sigma-Aldrich), N,N,N',N'-tetramethylethylenediamine (TEMED, 99%, as an accelerator), and ammonium persulfate (APS, 98%, as an initiator, Merck). The Nickel (II) chloride hexahydrate chemical (100%, NiCl₂·6H₂O) obtained from Merck prepared the solution containing 1000 ppm nickel ions. Okra was procured from the waste of local suppliers. The solution pH was adjusted by sodium hydroxide (100%, NaOH, Merck) and hydrochloric acid (37.5%, HCl, Sigma Aldrich) solutions. Additionally, distilled water (DI, 18.2 MΩ·cm; Human II-UV) was used throughout the experiment. The pH measurements were carried out with a Thermo Scientific pH meter. During sorption studies, UV-Vis spectroscopy (Thermo Scientific GENESYS 10S, USA) was used to quantify the amount of the drug.

Preparation of plant extract

Okra plants obtained from local suppliers were utilized for the synthesis of polymeric particles. The plants were homogenized in deionized water at a ratio of 1 g per 100 mL. The resulting homogenate was stirred using a magnetic stirrer at 50°C for 48 hours. After this extraction period, the solution was transferred into Falcon tubes and centrifuged at 9000 rpm for 20 minutes. The solid precipitate and liquid extract were separated through filtration. The aqueous okra extract was then collected in Falcon tubes and stored under refrigeration until further use in subsequent analyses [28].

Synthesis of polymeric particle based on okra/metal

Okra/metal-based polymeric particles were synthesized using a redox polymerization technique in an emulsion medium. Briefly, 10 mL of ethanol and 10 mL of deionized (DI) water were added to a 40 mL reaction vessel and mixed with a mechanical stirrer at 900 rpm for 10 minutes at room temperature. Subsequently, 2 mL of okra extract (10 g/100 mL) and 1 mL of EGDMA cross-linker (5.4×10^{-3} mol) were added to the reaction mixture, and stirring was continued until a homogeneous dispersion was obtained. Next, 1 mL of $\text{NiCl}_2 \cdot 6\text{H}_2\text{O}$ solution containing 1000 ppm of nickel ions was introduced, and the mixture was stirred for an additional 10 minutes at 900 rpm. To investigate the effect of metal ion concentration, particles were separately synthesized using nickel ion solutions at ten different concentrations (ranging from 100 to 1000 ppm), with the synthesis protocol repeated for each concentration. Once the components were thoroughly mixed, 40 μL of TEMED (accelerator) and 100 μL of APS solution (1×10^{-3} mol, initiator) were added to initiate polymerization. The reaction was allowed to proceed under continuous stirring with a magnetic stirrer for five hours at 25°C. Upon completion of polymerization, the mixture was transferred into centrifuge tubes and centrifuged at 9000 rpm for 30 minutes. The supernatant was discarded, and the solid particles were separated by filtration, washed with acetone, and dried in an oven at 40°C until a constant weight was achieved. The dried particles were stored in sealed containers for further analyses. The synthesis steps for the okra/Ni-based polymeric particles are schematically represented in Figure 1. The resulting particles were designated as p(Okra)/Ni, and a total of ten distinct polymeric particles were synthesized. Particles prepared with different concentrations of nickel ions (100, 200, 300, 400, 500, 600, 700, 800, 900, and 1000 ppm) were named p(Okra)/Ni₁, p(Okra)/Ni₂, p(Okra)/Ni₃, p(Okra)/Ni₄, p(Okra)/Ni₅, p(Okra)/Ni₆, p(Okra)/Ni₇, p(Okra)/Ni₈, p(Okra)/Ni₉, and p(Okra)/Ni₁₀, respectively [28].

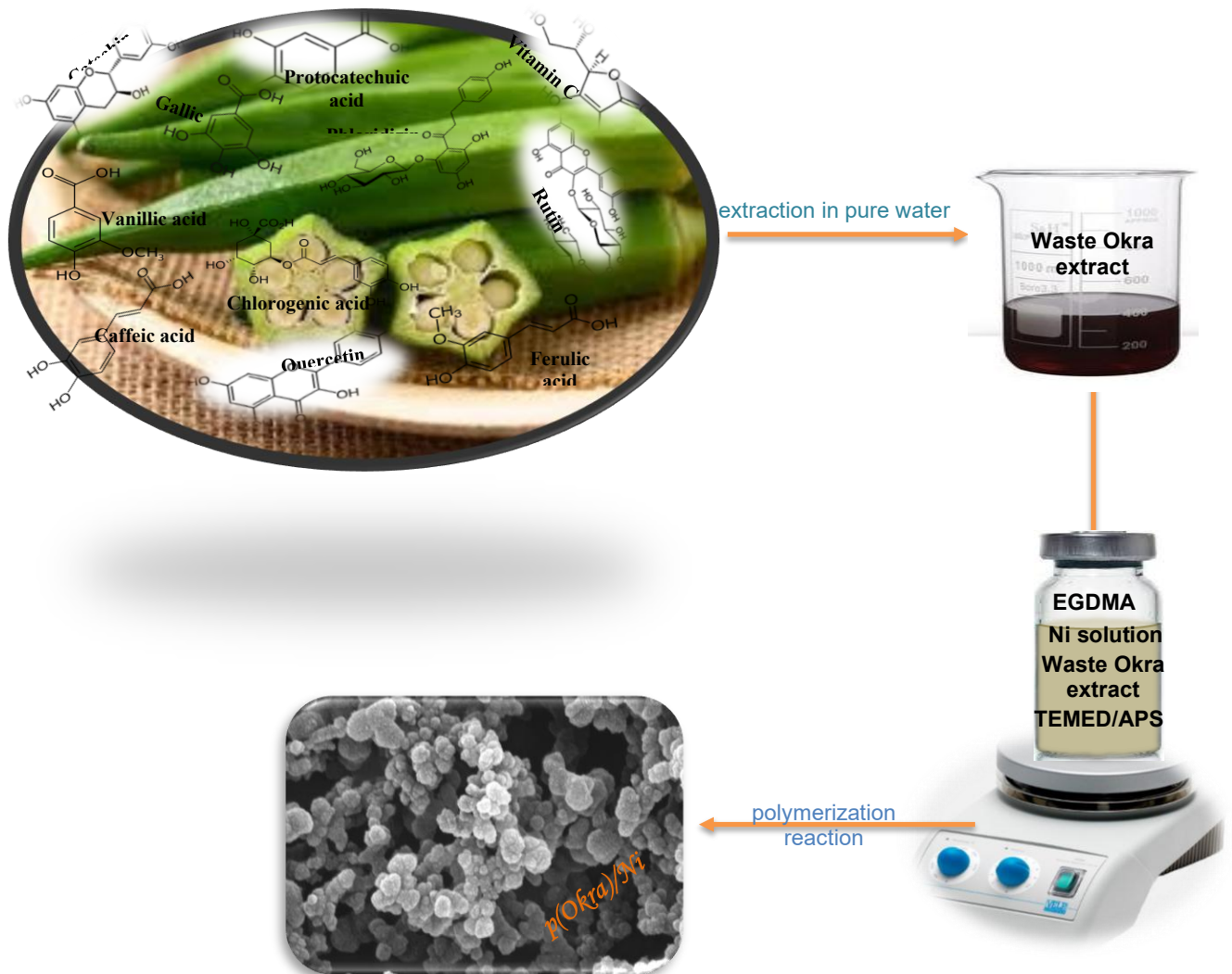


Figure 1. The scheme of p(Okra)/Ni particle preparation.

Characterization of p(Okra)/Ni-based particle

The structural properties of the synthesized particles were examined using various analytical instruments.

Sorption experiments

In this study, ten different p(Okra)/Ni-based polymeric particles were synthesized via a redox polymerization technique, utilizing waste okra and nickel ion solutions at varying concentrations. These particles were systematically evaluated for their sorption performance in removing acetaminophen from aqueous solutions. Batch sorption experiments were conducted in triplicate to ensure data reliability. In the initial phase, the sorption efficiency of all ten p(Okra)/Ni particle types was screened under identical conditions. Key experimental parameters were held constant as follows: acetaminophen concentration (50 mg/L), temperature (25°C), stirring speed (900 rpm), solution pH (6.5, deionized water), contact time (24 hours), and particle dosage (0.2 mg/mL). Based on this preliminary assessment, p(Okra)/Ni₁ and p(Okra)/Ni₃ were identified as the most effective sorbents for acetaminophen removal. Subsequently, the effects of particle dosage and initial acetaminophen concentration were investigated, while all other parameters were kept unchanged. To assess the influence of particle dosage, the amount of sorbent was varied between 2.5 mg and 50 mg. For the effect of acetaminophen concentration, the particle-to-solution ratio was fixed at 0.05 mg/mL, with acetaminophen concentrations ranging from 10 mg/L to 200 mg/L. Following the optimization of sorbent type, dosage, and pollutant concentration, the impact of pH and temperature on sorption efficiency was further studied. The pH was adjusted between 3 and 9 using 0.1 M NaOH and 0.1 M HCl, while temperature effects were examined in the range of 10°C to 50°C. These tests were conducted at pH 5, using a particle concentration of 0.05 mg/mL, and stirred at 900 rpm for 24 hours. Each parameter (particle type, acetaminophen concentration, particle amount, pH, and temperature) was evaluated independently to determine its influence on acetaminophen sorption. The optimum experimental conditions were determined as follows: p(Okra)/Ni₁ or p(Okra)/Ni₃, acetaminophen concentration of 50 mg/L, particle amount of 2.5 mg, pH 5, and temperature of 30°C. The residual acetaminophen concentration in solution was quantified using UV-Vis spectrophotometry at 240 nm. Equilibrium sorption capacity (q_e , mg/g) was calculated according to standard procedures reported in the literature [30].

$$q_e = \frac{(C_o - C_e) \cdot V}{M} \quad (1)$$

or

$$\text{Removal efficiency (\%)} = \frac{(C_o - C_t)}{C_o} \cdot 100 \quad (2)$$

where C_o represents the initial concentration of acetaminophen (mg/L); C_e is the equilibrium concentration of acetaminophen (mg/L); C_t is the concentration at a certain time t (or at equilibrium) (mg/L); V represents the solution volume (L); and M is the particle mass (g).

Sorption isotherms, and thermodynamic parameters

Sorption isotherms describe the relationship between the amount of solute sorbed by a sorbent material and the solute concentration in the liquid phase at a constant temperature. These isotherms are widely used to investigate sorption behavior and to design and optimize sorption processes in various applications, including air and water purification, gas separation, and catalysis. Commonly applied models to describe sorption isotherms include the Langmuir (Eq. (3)) [31], Freundlich (Eq. (4)) [32], **Tempkin** (Eq. (5)) [33], and Dubinin-Radushkevich isotherms (Eq. (6)) [34]. Each model is based on different assumptions about the sorption system and has its own limitations. The equations for the isotherm models used in this study to analyze equilibrium sorption data are provided in Table 1.

Sorption thermodynamic parameters quantify the thermodynamic properties of a system undergoing sorption. Sorption refers to the process by which a substance, such as a gas or liquid, binds to the surface of another substance, typically a solid. The most commonly used sorption thermodynamic parameters are the Gibbs free energy change (ΔG°), enthalpy change (ΔH°), and entropy change (ΔS°). These parameters were calculated using Equations (7), (8), and (9) [35-36].

$$K^0 = \frac{C_t}{C_e} \quad (7)$$

$$\Delta G^0 = \Delta H^0 - T \cdot \Delta S^0 \quad (8)$$

$$\ln K^0 = \frac{\Delta S^0}{R} - \frac{\Delta H^0}{R \cdot T} \tag{9}$$

where K^0 is a constant related to sorption equilibrium; C_t is the sorbed acetaminophen concentration at the time t (mg/L). The ΔH^0 and ΔS^0 values were achieved from the slope and intercept of Van't Hoff plots of $\ln K^0$ vs. $1/T$.

Table 1. Sorption isotherm models for acetaminophen sorption.

Model	Mathematical Equation
Langmuir (L) (Eq. 3)	$\frac{C_e}{q_e} = \left(\frac{C_e}{q_{max}}\right) + \left(\frac{1}{q_{max} \cdot K_L}\right)$
Freundlich (F) (Eq. 4)	$\log q_e = \log K_f + \left(\frac{1}{n}\right) \log C_e$
Tempkin (T) (Eq. 5)	$q_e = \frac{R \cdot T}{b_T} \ln A_T + \left(\frac{R \cdot T}{b_T}\right) \ln C_e$
Dubinin–Radushkevich (D–R) (Eq. 6)	$\ln q_e = \ln q_s - \beta \cdot \varepsilon^2$ $\varepsilon = R \cdot T \cdot \ln \left(1 + \frac{1}{C_e}\right)$ $E = \frac{1}{\sqrt{2 \cdot \beta}}$

Results and Discussion

Characterization of synthesized particle

Polymeric particles synthesized from p(Okra) and p(Okra)/Ni for potential drug sorption applications were characterized using various analytical techniques to determine their structural and surface properties. The aim of these analyses was to identify the key characteristics of the particles and to evaluate the effects of nickel ion incorporation into the polymer matrix. Understanding these properties is essential for assessing the suitability of the materials for specific applications. In this context, Scanning Electron Microscopy (SEM) was used to investigate surface morphology, while Thermogravimetric Analysis and Differential Scanning Calorimetry (TGA/DSC) were employed to assess thermal stability and degradation behavior. Furthermore, the Brunauer–Emmett–Teller (BET) method was used to evaluate surface area and pore structure, and dynamic light scattering (DLS), along with zeta potential measurements, provided insights into particle size and colloidal stability. Fourier Transform Infrared Spectroscopy (FT-IR) was used to identify chemical bonds and functional groups. The data obtained from these analyses provided a comprehensive understanding of the structural characteristics of the particles, offering valuable insights for their potential use in future applications.

Scanning electron microscopy (SEM)

The morphological structures of the p(Okra) and p(Okra)/Ni-based polymeric particles were examined using Scanning Electron Microscopy (SEM), and representative images are presented in Figure 2. As shown in Figure 2a, the surface of the p(Okra) particles appears generally porous, exhibiting a multilayered spherical morphology with small surface crevices. Such a porous and irregular surface structure is favorable for drug sorption, as it offers increased surface area and more potential binding sites for drug molecules. However, the observed tendency of these particles to agglomerate may negatively impact their dispersibility and reduce the effective surface area available for sorption, particularly in aqueous or biological environments. In Figures 2b and 2c, the incorporation of Ni ions into the polymeric matrix retains the general morphological features of the p(Okra) particles while introducing additional surface roughness in the form of small, bubble-like protrusions. Moreover, a reduction in average particle size was observed. This nanoscale surface texturing and size reduction can enhance the interaction between drug molecules and the particle surface by increasing surface-to-volume ratio, thereby potentially improving sorption efficiency. Interestingly, increasing the Ni ion concentration from 100 ppm to 1000 ppm further intensified surface roughness and appeared to yield more compact and less aggregated particles. **Such morphological modifications provide greater structural integrity and a higher accessible surface area, which are essential for maximizing drug-loading efficiency and sustaining drug retention.** However, excessive incorporation of metal ions may alter surface chemistry in ways that affect biocompatibility or lead to nonspecific interactions with drug molecules, potentially reducing sorption selectivity or increasing cytotoxicity, depending on the application. Overall, the SEM analysis confirmed the successful incorporation of metal ions into the polymeric structure and

highlighted morphological characteristics that could positively influence the drug sorption capacity of the particles.

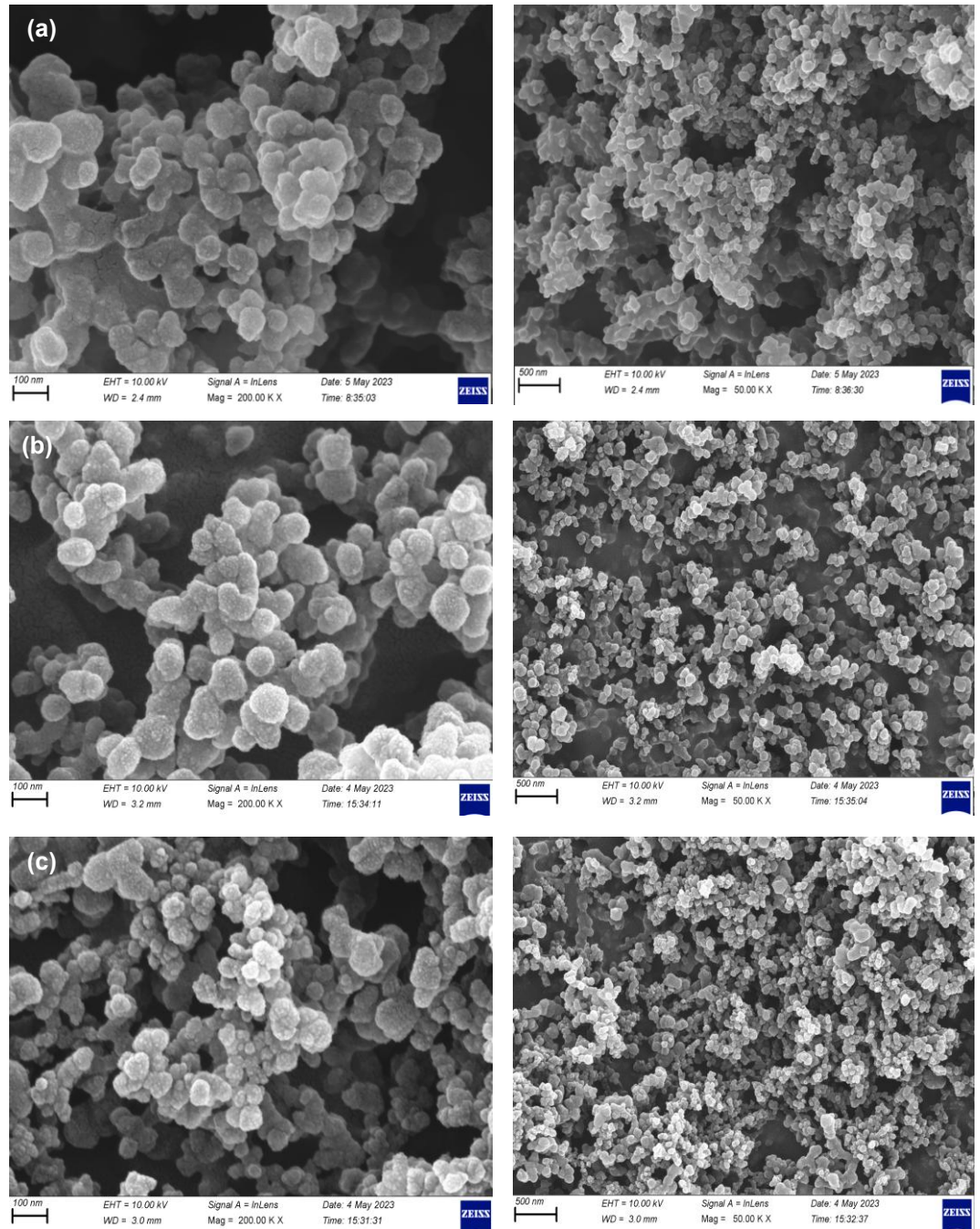


Figure 2. The SEM images of (a) p(Okra), (b) p(Okra)/Ni₁ and (c) p(Okra)/Ni₁₀ particles.

Thermogravimetric analysis (TGA/DSC)

The thermal degradation behavior of p(Okra) and p(Okra)/Ni particles was analyzed using a TGA/DSC analyzer, as shown in Figure 3. Thermogravimetric analysis (TGA) provides insight into the thermal stability and decomposition characteristics of polymeric materials by monitoring mass loss over a temperature range. Both p(Okra) and p(Okra)/Ni₁₀ particles exhibited nearly complete degradation (~100% mass loss) upon heating to 1000°C under an argon atmosphere, reflecting their organic composition and biodegradability. For the p(Okra)/Ni₁₀ particles, five distinct degradation stages were observed. The initial mass loss of 2.99% between 50 and 144°C was attributed to the evaporation of

adsorbed moisture and low-molecular-weight volatiles. The second (144–233°C, 6.13%) and third (233–295°C, 7.66%) stages likely correspond to the thermal decomposition of hemicellulose-like structures and polysaccharide chains. Major degradation occurred in the fourth (295–386°C, 42.74%) and fifth (386–447°C, 40.48%) stages, associated with the breakdown of the polymer backbone and cross-linked matrix. In comparison, p(Okra) particles displayed a broader degradation profile: 22% mass loss between 50 and 250°C, 16% between 250 and 320°C, 42% between 320 and 386°C, and 20% up to 418°C. The earlier onset and more gradual degradation pattern of p(Okra) indicate relatively lower thermal stability. The incorporation of Ni ions significantly altered the thermal degradation pathway, likely due to enhanced cross-linking or metal–ligand interactions within the polymer matrix. This modification contributed to a more defined multi-step degradation pattern and improved thermal stability. These findings underscore the structural reinforcement provided by Ni ions, which may enhance the applicability of the synthesized particles under environmental conditions involving thermal or chemical stress.

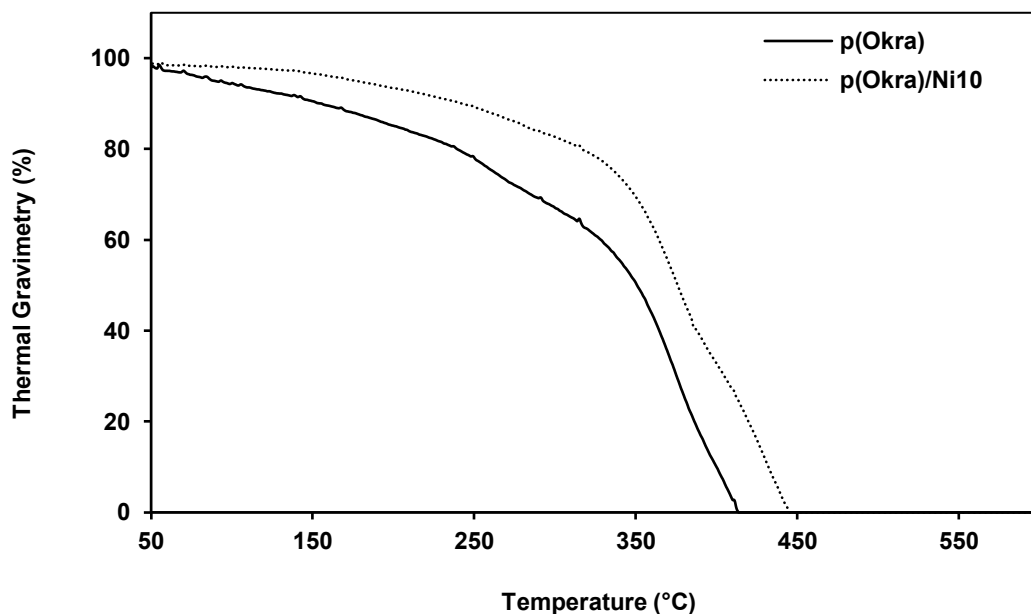


Figure 3. Thermal behavior of p(Okra), and p(Okra)/Ni₁₀ particles.

Brunauer–emmett–teller surface area meter (BET)

The surface area and porosity characteristics of the synthesized particles were investigated using nitrogen adsorption–desorption isotherms via the BET method. The specific surface areas of p(Okra), p(Okra)/Ni₁, and p(Okra)/Ni₁₀ were found to be relatively similar, ranging from approximately 83.7 to 88.4 m²/g, while a slight increase in pore volume and average pore diameter was observed with increasing Ni content (Table 2). For drug sorption applications, surface area and pore structure directly influence the loading capacity and diffusion kinetics of drug molecules. Although the overall BET surface area did not change significantly, the increased pore volume and diameter in Ni-modified particles may enhance drug uptake by providing more accessible internal spaces for adsorption. Mesoporous structures are especially beneficial for the loading of moderately sized drug molecules. However, if the pores are too large, premature release or reduced retention may occur. Thus, the ability to fine-tune porosity through Ni incorporation offers a valuable tool for optimizing drug delivery profiles tailored to specific active compounds.

Particle size and zeta potential measurement device (Zeta-DIs)

Zeta potential measurements provide insights into particle stability based on the electrical double layer formed around the particles. When particles possess a uniform charge, they repel each other, preventing aggregation and thus maintaining stability. Conversely, low zeta potential values indicate a tendency toward agglomeration. The zeta potentials of p(Okra), p(Okra)/Ni₁, and p(Okra)/Ni₁₀ particles were measured as -1.05 mV, -0.00113 mV, and -0.541 mV, respectively, indicating a tendency for these particles to cluster. The particle sizes of the synthesized p(Okra), p(Okra)/Ni₁, and p(Okra)/Ni₁₀ were measured as 226.6 nm, 288.8 nm, and 638.4 nm, respectively. Therefore, the sizes of the synthesized particles ranged from approximately 100 nanometers to 100 micrometers, categorizing them as microsized particles.

Table 2. Pore structure characterization of p(Okra) and p(Okra)/Ni particles.

Sorbent	BET Surface Area (m ² /g)	BJH Pore Volume (cm ³ /g)	BJH Pore Diameter (nm)
p(Okra)	86.89	0.27	11.16
p(Okra)/Ni ₁	88.38	0.29	12.45
p(Okra)/Ni ₁₀	83.71	0.33	14.08

Fourier transform infrared spectrophotometer (FT-IR)

FT-IR spectroscopy was utilized to investigate the possible chemical structures and bonding interactions within the synthesized p(Okra)/Ni-based polymeric particles. The spectra of particles cross-linked with EGDMA were recorded over the range 4000–500 cm⁻¹ (Figure 4). According to literature on natural fiber FT-IR analysis, okra fibers typically exhibit a broad –OH stretching band around 3600–3100 cm⁻¹, attributed to hydroxyl groups present in cellulose and hemicellulose [37]. In our samples, this –OH band notably diminished after polymerization, which may indicate consumption or involvement of hydroxyl groups in new hydrogen bonding or covalent linkages during cross-linking with EGDMA, as similarly reported for other biopolymer composites [38]. Characteristic peaks observed near 2972 cm⁻¹ and 2900 cm⁻¹ correspond to C–H stretching vibrations of aliphatic groups,

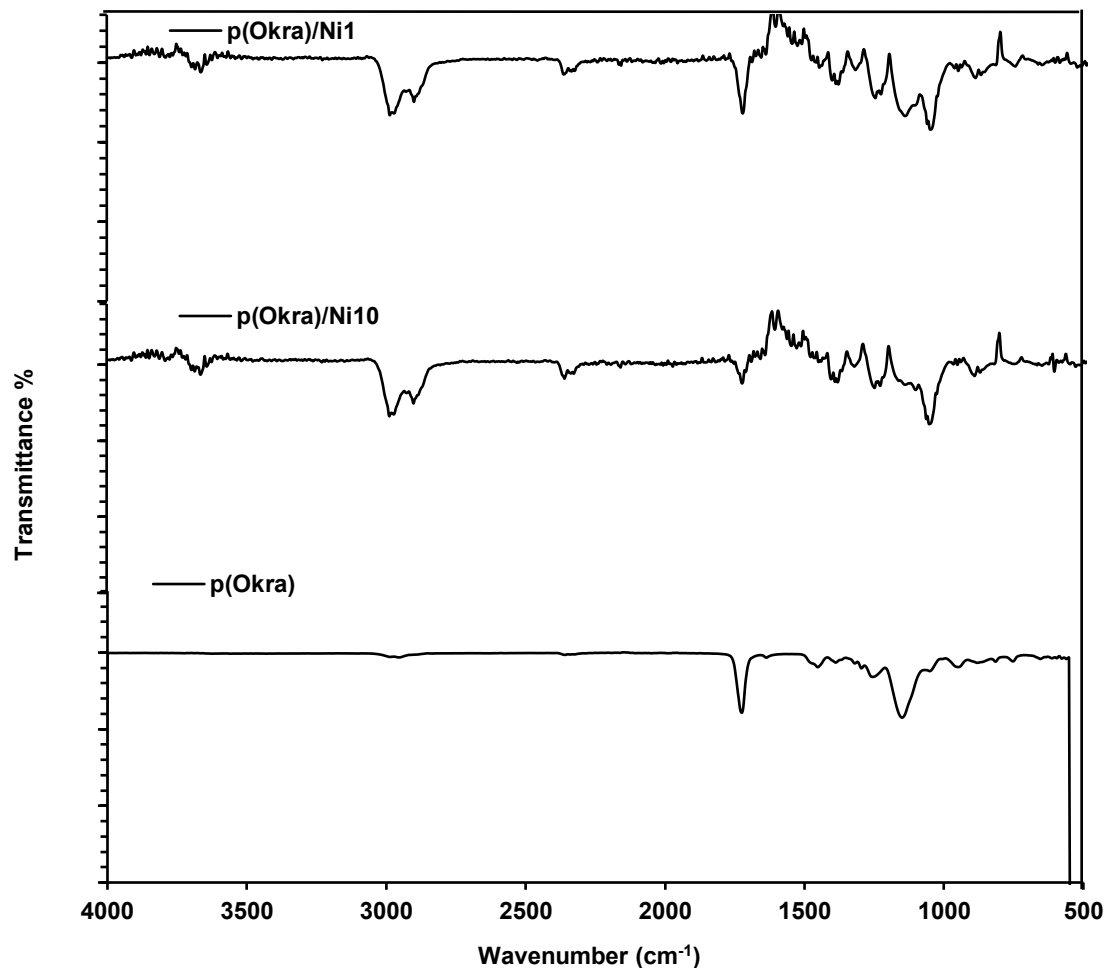


Figure 4. FT-IR spectra of p(Okra), p(Okra)/Ni₁ and p(Okra)/Ni₁₀ particles.

consistent with the literature on polymeric materials containing alkyl chains [39]. The absorption band at approximately 1724 cm⁻¹ can be attributed to the C=O stretching vibrations of ester groups in EGDMA or possibly carboxylic acid groups in lignin or hemicellulose, aligning with previous studies on esterified natural polymers. Bands detected around 1450 cm⁻¹ and 1145 cm⁻¹ likely represent C–H bending vibrations of alkanes and C–O stretching vibrations of ester functionalities, respectively, as commonly observed in cross-linked polymer systems [40]. Furthermore, the appearance of new peaks at 1381 cm⁻¹ and 1230 cm⁻¹ in particles cross-linked with Ni ions suggests possible coordination interactions or formation of new chemical bonds involving the nickel centers, similar to observations reported in metal-polymer complexes [41-42].

Acetaminophen drug sorption

Research indicates that the body is unable to utilize over 50% of the prescribed acetaminophen dose during therapeutic use [43]. As a result, the unmetabolized portion is excreted via urine or feces and subsequently released into the environment. Over time, the accumulation of residual acetaminophen may pose significant environmental risks, making it a subject of growing ecological concern. In this study, the effect of p(Okra)/Ni particles on the removal of acetaminophen was thoroughly investigated, considering variables such as particle type, particle dosage, initial acetaminophen concentration, pH, and temperature.

Effect of sorbent type

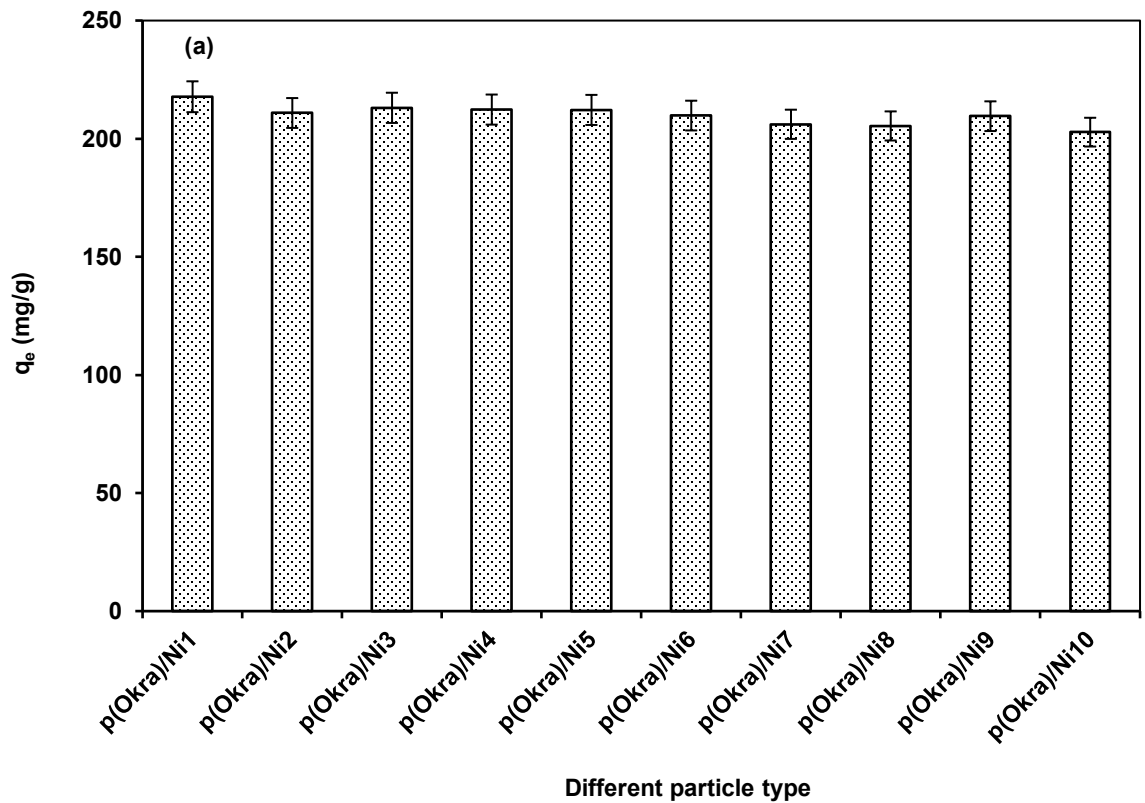
As shown in Figure 5a, the particle exhibiting the highest acetaminophen removal capacity was p(Okra)/Ni₁, which was synthesized using a solution containing 100 ppm of Ni ions, achieving a maximum acetaminophen removal of 217.7 mg/g. Other particles demonstrated comparable sorption characteristics, though to a slightly lesser extent. Acetaminophen is known to have a pKa value of approximately 9.38. Therefore, in an aqueous solution, the protonated or neutral form predominates at pH values below the pKa, while the deprotonated form becomes dominant above pH 9.38 [44]. According to zeta potential measurements, the surface charge of the particles was observed to be negative. Since the pH of the solution in this study was approximately 6.5, acetaminophen would predominantly exist in its neutral form, which may facilitate electrostatic or hydrogen bonding interactions with the negatively charged particle surface, thereby enhancing sorption efficiency.

Effect of sorbent dosage

The amount of sorbent used in sorption experiments plays a critical role in the removal efficiency of the target compound. To assess this effect, the sorbent mass was varied between 0.0025 and 0.05 g, while maintaining constant experimental conditions, including an initial acetaminophen concentration of 50 mg/L, room temperature, and neutral pH. The influence of sorbent dosage on acetaminophen uptake by p(Okra)/Ni₁ and p(Okra)/Ni₃ particles was examined, and the results are presented in Figure 5b. The highest acetaminophen sorption capacity was obtained using 0.0025 g of sorbent. Under these conditions, the amount of acetaminophen adsorbed per gram of p(Okra)/Ni₁ and p(Okra)/Ni₃ was calculated as 592.1 mg/g and 566.1 mg/g, respectively. The observed decrease in sorption capacity with increasing sorbent dose can be explained by the "concentration gradient (or flux) splitting effect", which reduces the driving force for mass transfer per unit sorbent. As a result, the amount of acetaminophen sorbed per gram of sorbent decreases, leading to a reduction in sorption density. Additionally, interparticle interactions, such as aggregation at higher sorbent concentrations, may also contribute to this decline. Such aggregation can lead to a decrease in accessible surface area and an increase in diffusion path length, thereby negatively affecting the overall sorption performance [45].

Effect of initial acetaminophen concentration

Sorption tests were conducted at various initial acetaminophen concentrations (10, 25, 50, 75, 100, and 200 mg/L) to investigate the effect of concentration on sorption performance. The sorbent-to-solution ratio was maintained at 0.05 mg/mL throughout the experiments. The variation in acetaminophen uptake per gram of p(Okra)/Ni₁ and p(Okra)/Ni₃ particles at different initial concentrations is illustrated in Figure 6a. As shown in the figure, acetaminophen uptake increased with rising initial concentration, indicating enhanced mass transfer due to a stronger concentration gradient. However, beyond a certain concentration, the rate of increase in sorption began to plateau, suggesting that the available active sites on the sorbent surface were approaching saturation. The maximum sorption capacities were determined as 507.6 mg/g for p(Okra)/Ni₁ and 452.2 mg/g for p(Okra)/Ni₃. The primary driving force for sorption is the concentration gradient, which facilitates mass transfer of drug molecules from the solution to the sorbent surface. At low concentrations, sorption is limited due to the weaker driving force, whereas higher concentrations enhance the diffusion of acetaminophen toward the sorbent surface. However, once sorption equilibrium is reached, no significant increase in uptake occurs, regardless of further increases in concentration. Additionally, since the stirring speed remained constant, it was inferred that the observed variations in uptake were primarily governed by concentration-dependent diffusion rather than external mass transfer resistance. This highlights the critical role of initial drug concentration in influencing sorption kinetics and capacity.



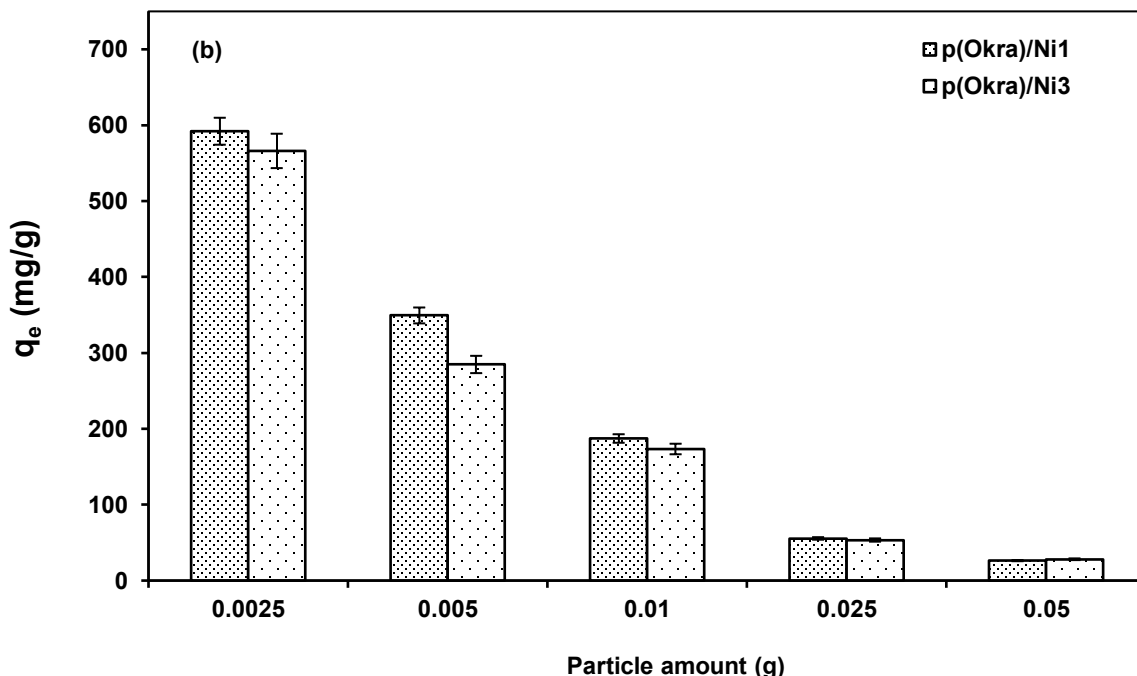


Figure 5. (a) Effect of p(Okra)/Ni-based particle type on acetaminophen sorption and (b) Effect of p(Okra)/Ni-based particle amount on acetaminophen sorption.

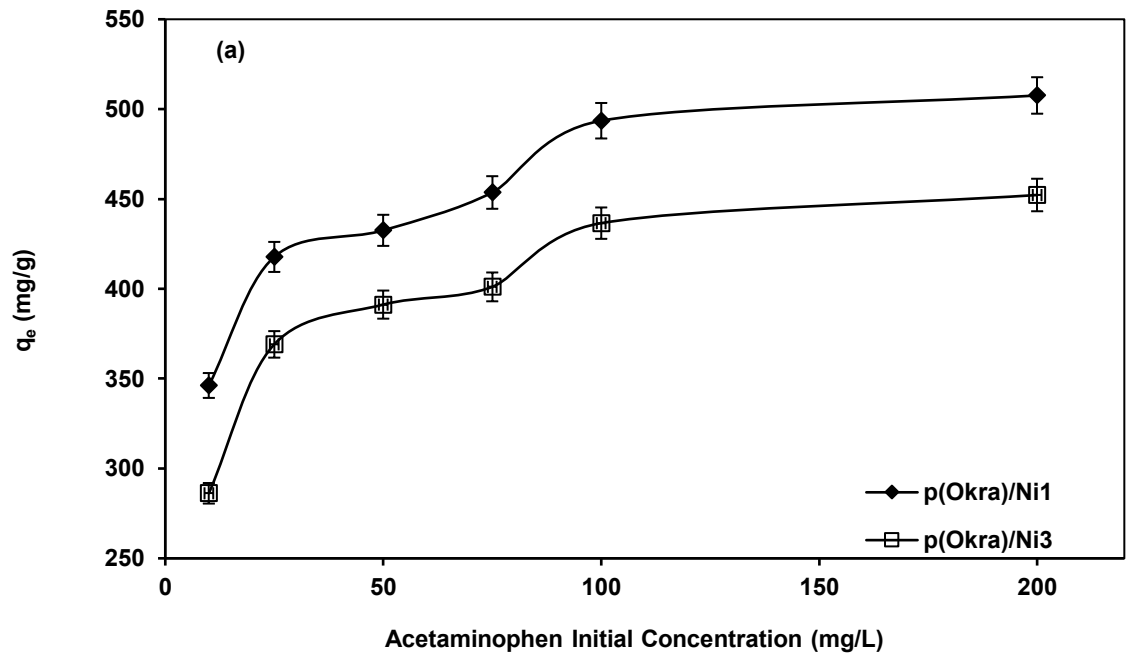
Effect of pH on acetaminophen sorption

The influence of solution pH on acetaminophen sorption was investigated using p(Okra)/Ni₁ and p(Okra)/Ni₃ particles under constant conditions: room temperature, 50 mL solution volume, and an initial acetaminophen concentration of 50 mg/L. The pH of the solution was adjusted to 3, 5, 7, and 9, and the variation in acetaminophen uptake per gram of sorbent is shown in Figure 6b. As illustrated in the figure, solution pH had a significant effect on sorption capacity. The highest uptake was observed at pH 7, where the maximum sorption capacity reached 331.3 mg/g for p(Okra)/Ni₁ and 308.9 mg/g for p(Okra)/Ni₃ particles. Acetaminophen has a pK_a value of 9.38. Therefore, in aqueous solutions, the neutral (protonated) form of the drug predominates when the pH is below 9.38, while the anionic (deprotonated) form predominates at pH values above 9.38 [44]. Since the experiments were conducted within the pH range of 3 to 9, acetaminophen primarily existed in its neutral form, particularly near pH 7, which likely facilitated favorable non-ionic interactions. Based on these findings, it is suggested that hydrogen bonding plays a more dominant role than electrostatic interactions in the sorption mechanism of acetaminophen onto p(Okra)/Ni-based particles. The observed pH dependence supports the hypothesis that surface functional groups of the biopolymer, particularly hydroxyl or ester moieties, interact with acetaminophen through hydrogen bonding, which is most effective under near-neutral pH conditions.

Effect of temperature on sorption behavior

The effect of temperature on the sorption of acetaminophen by p(Okra)/Ni₁ and p(Okra)/Ni₃ particles was evaluated in 50 mL of aqueous solution containing 50 mg/L acetaminophen, at two pH values (7 and 9). As illustrated in Figure 6c, the amount of acetaminophen adsorbed per gram of sorbent varied with temperature. For p(Okra)/Ni₁, the maximum sorption capacity was recorded as 280.7 mg/g at 30 °C and pH 9, while p(Okra)/Ni₃ exhibited a peak sorption capacity of 263 mg/g at 20 °C under the same pH conditions. These observations suggest that temperature has a notable impact on sorption behavior, influencing both the extent and efficiency of drug uptake.

To further understand the sorption mechanism, thermodynamic parameters, enthalpy change (ΔH°), entropy change (ΔS°), and Gibbs free energy change (ΔG°), were calculated using Equations 7–9, and the corresponding results are presented in Table 3. The negative values of ΔH° for both sorbents confirm that the acetaminophen sorption process is exothermic in nature. Furthermore, the negative ΔS° values indicate a decrease in system randomness at the solid–liquid interface during sorption, implying an increase in structural order as acetaminophen molecules associate with the polymer surface. Interestingly, the positive ΔG° values obtained at the tested temperature range imply that the sorption process is non-spontaneous under these experimental conditions. This thermodynamic profile suggests that while the process is energetically favorable in terms of enthalpy, the loss of entropy outweighs the enthalpic gain, resulting in a net thermodynamic penalty. Additionally, as temperature increases beyond the optimal point (e.g., $>30^\circ\text{C}$), sorption efficiency decreases, likely due to the desorption of weakly bound acetaminophen molecules or disruption of hydrogen bonding interactions. In summary, the



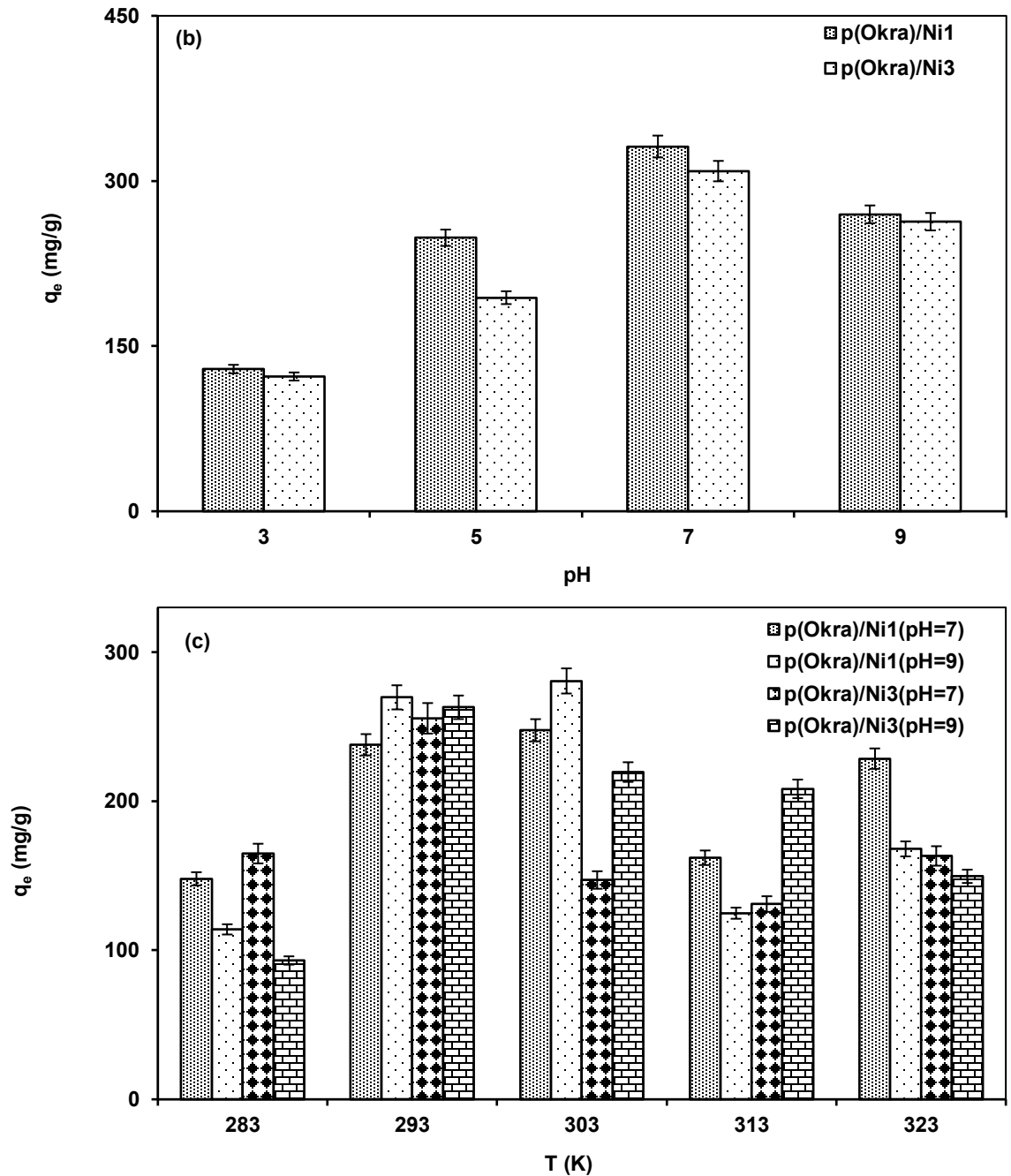


Figure 6. (a) Effect of acetaminophen initial concentration on acetaminophen sorption, (b) Effect of pH on acetaminophen sorption and (c) Effect of temperature on acetaminophen sorption.

sorption of acetaminophen onto p(Okra)/Ni-based particles is exothermic and entropy-reducing, and exhibits temperature sensitivity, indicating that lower to moderate temperatures are more suitable for achieving efficient drug removal under the given pH conditions [46].

Sorption isotherms

The sorption behavior of acetaminophen onto p(Okra)/Ni₁ and p(Okra)/Ni₃ particles was evaluated using four isotherm models: Langmuir, Freundlich, **Tempkin**, and Dubinin–Radushkevich (D–R). The model parameters obtained from linear regression analyses are summarized in Table 4. According to the Langmuir isotherm, the data suggest monolayer sorption on a homogeneous surface, where all sorption sites have equal affinity for the sorbate. This model assumes no interactions between adsorbed

molecules, making it suitable for describing uniform adsorption sites. The higher correlation coefficients (R^2) obtained for both $p(\text{Okra})/\text{Ni}_1$ and $p(\text{Okra})/\text{Ni}_3$ in the Langmuir model, compared to the other models, indicate that this model best fits the experimental data. Consequently, it can be inferred that acetaminophen sorption predominantly occurs on structurally homogeneous regions of the polymer surfaces. The Freundlich isotherm, which is an empirical model, reflects surface heterogeneity and variation in adsorption site energies. The Freundlich constant (n) values for $p(\text{Okra})/\text{Ni}_1$ and $p(\text{Okra})/\text{Ni}_3$ were found to be 12.5 and 8.8, respectively. These high n values ($n > 1$) imply favorable sorption conditions and confirm that the synthesized particles are efficient sorbents for acetaminophen. The **Tempkin** isotherm, which considers sorbent–sorbate interactions and assumes a linear decrease in the heat of adsorption with coverage, yielded lower R^2 values. Similarly, the Dubinin–Radushkevich (D–R) isotherm, typically applied to porous and heterogeneous materials with Gaussian energy distributions, also exhibited poor fitting, as indicated by its low correlation coefficients [47-49]. These findings suggest that neither the **Tempkin** nor the D–R model adequately describes the sorption mechanism for these systems. The maximum theoretical sorption capacities derived from the Langmuir model were 500 mg/g for $p(\text{Okra})/\text{Ni}_1$ and 454.6 mg/g for $p(\text{Okra})/\text{Ni}_3$, which are in good agreement with the experimentally determined values, further validating the model's applicability [50].

Table 3. Thermodynamic parameters for sorption of acetaminophen by particles.

Particles	pH	Temperature (K)	ΔG° (J/mol)	ΔH° (J/mol)	ΔS° (J/(mol*K))
$p(\text{Okra})/\text{Ni}_1$	7	283	2858.8	-16764.3	-69.4
		293	3552.2		
		303	4245.5		
		313	4938.9		
		323	5632.3		
$p(\text{Okra})/\text{Ni}_1$	9	283	2949.8	-10841.5	48.7
		293	3437.2		
		303	3924.5		
		313	4411.8		
		323	4899.1		
$p(\text{Okra})/\text{Ni}_3$	7	283	2968.5	-20663.6	-83.5
		293	3803.6		
		303	4638.6		
		313	5473.7		
		323	6308.8		
$p(\text{Okra})/\text{Ni}_3$	9	283	2862.9	-13603.4	-58.2
		293	3444.8		
		303	4026.6		
		313	4608.4		
		323	5190.3		

To assess the comparative performance of the synthesized $p(\text{Okra})/\text{Ni}$ particles, their maximum sorption capacities were benchmarked against other acetaminophen sorbents reported in the literature (Table 5) [12, 28, 51-57]. The results demonstrate that $p(\text{Okra})/\text{Ni}$ -based materials exhibit competitive or superior performance, positioning them as promising candidates for pharmaceutical contaminant removal from aqueous media. Furthermore, the use of okra biomass, an agricultural waste product, provides an added benefit of waste valorization, contributing to both sustainable waste management and economic value creation. Nevertheless, it is important to note that variability in experimental conditions, such as pH, temperature, initial drug concentration, and contact time, across different studies can limit direct comparison of performance metrics. Despite these limitations, all sorbents present distinct advantages and constraints, and the applicability of each material depends on specific environmental and operational parameters.

Table 4. Isotherm results for sorption of acetaminophen by particles.

Model		Particles	
		p(Okra)/Ni ₁	p(Okra)/Ni ₃
Langmuir Isotherm Constants	K _L (L/mg)	0.25	0.16
	q _m (mg/g)	500	454.6
	R ²	0.9979	0.9956
Freundlich Isotherm Constants	K _f	333.1	254
	n	12.5	8.8
	R ²	0.933	0.8917
Tempkin Isotherm Constants	b _T	73.7	59.5
	A _T (L/g)	16411.3	299.3
	R ²	0.9257	0.9128
Dubinin-Radushkevich Isotherm Constants	E (kJ/mol)	1.29	0.5
	R ²	0.7395	0.8801

Table 5. Comparison of the sorption capacities (maximum sorption capacity or maximum Langmuir sorption capacity) of some sorbents in the literature for acetaminophen sorption.

Sorbents	Conditions	Sorption (mg/g)	References
SAC from jatobá	pH = 5, T = 303K	356.25	[12]
p(Okra)/Fe ₃	pH=6.5, time = 24 h, T=298K, sorbent dosage = 0.05 g L ⁻¹ , C ₀ =10-200 mg L ⁻¹	869.4	[28]
p(Okra)/Fe ₈		854.7	
Banana Peel biochar (BPBC750)	pH=3, T=283K-298K-313K, C ₀ =0.5-100 mg L ⁻¹	40.83 (283K)	[51]
		49.43 (298K)	
		57.26 (313K)	
superparamagnetic activated carbons (SPACs)	pH = 3-10, C ₀ =25-500 mg L ⁻¹	234.3	[52]
Activated carbon from <i>Butia capitata</i>	pH = 7, T = 298K	100.6	[53]
Spiky green horse-chestnut shell	pH=6, time = 10 min, sorbent dosage = 0.5 g, C ₀ = 50 mg L ⁻¹	1.48	[54]
Iron/bentonite/eggshell	time = 150 min, C ₀ =10-100 mg L ⁻¹	469	[55]
Bentonite/eggshell	time = 50 min, C ₀ =10-100 mg L ⁻¹	400	[55]
Fruit of Butiacapitate AC	pH = neutral, time = 20 min, T = 298-328 K, sorbent dosage = 0.9 g/L, C ₀ = 50-300 mg L ⁻¹	98.19	[56]
MCM-41-GO	time = 200 min, C ₀ =200 mg L ⁻¹	322.6	[57]
MCM-41-G	time = 220 min, C ₀ =200 mg L ⁻¹	555.6	[57]
ASM41	time = 30 min, C ₀ =200 mg L ⁻¹	121.9	[57]
p(Okra)/Ni ₁	pH=6.5, time = 24 h, T=298K, sorbent dosage = 0.05 g L ⁻¹ , C ₀ =10-200 mg L ⁻¹	507.6	This work
p(Okra)/Ni ₃		452.2	

Clarification of the mechanism of acetaminophen sorption

A general sorption mechanism for acetaminophen onto p(Okra)/Ni particles can be proposed by taking into account the physicochemical characteristics of the sorbent, such as surface morphology, functional group diversity, and porosity, alongside the chemical structure and behavior of acetaminophen under different environmental conditions (Figure 7). The pH-dependent nature of acetaminophen sorption, as observed in experimental data, suggests that electrostatic interactions are not the dominant mechanism.

However, the incorporation of Ni ions into the polymer matrix may locally enhance electrostatic attractions through partial positive charges, thereby contributing to sorption in a secondary manner. The surface of p(Okra)/Ni particles contains a variety of polar functional groups (e.g., $-\text{OH}$, $-\text{COOH}$, and carbonyl moieties), enabling the formation of multiple interaction types with acetaminophen molecules. The following interactions are likely responsible for the observed sorption behavior:

- π - π interactions: Acetaminophen contains a phenyl ring that can participate in π - π stacking with aromatic domains present in the polymer matrix. The aromatic rings in both the drug and the p(Okra)/Ni structure enable this interaction, particularly under acidic to neutral pH where aromatic stabilization is more favorable.
- n - π electron donor-acceptor interactions: The lone electron pairs (n) on oxygen atoms in surface carbonyl groups of the sorbent can interact with the π orbitals* of acetaminophen's benzene ring. This donor-acceptor mechanism facilitates close contact and alignment of acetaminophen on the sorbent surface.
- Hydrogen bonding (H-bonding): One of the most significant interactions identified is hydrogen bonding, supported by previous studies on acetaminophen sorption mechanisms [58-59]. The $-\text{OH}$ and $-\text{NH}$ groups of acetaminophen serve as hydrogen bond donors, while the polar groups on p(Okra)/Ni, such as $-\text{OH}$ and $-\text{COOH}$, can act as both donors and acceptors. These bonds promote stable binding and contribute to the selectivity of the sorbent.
- Pore filling: The well-developed porous structure of the p(Okra)/Ni particles provides physical entrapment sites for acetaminophen molecules. The molecule's relatively small size enables it to diffuse into both mesoporous and microporous regions, where van der Waals forces and capillary effects further assist retention. This pore-filling effect becomes particularly relevant at higher acetaminophen concentrations, where surface interactions may be saturated.

Furthermore, under acidic pH conditions, acetaminophen exhibits a resonance-stabilized nitrogen lone pair, which acts as a π -donor, enhancing π -based interactions with the sorbent [58-59]. This behavior underscores the importance of pH modulation in optimizing interaction types. Taken together, these findings suggest that acetaminophen sorption onto p(Okra)/Ni particles is governed by a multimechanistic pathway, primarily dominated by hydrogen bonding, π - π stacking, and n - π donor-acceptor interactions, with pore diffusion and weak electrostatic attractions playing auxiliary roles. This multifaceted sorption mechanism accounts for the high capacity and efficiency observed in the removal experiments [60].

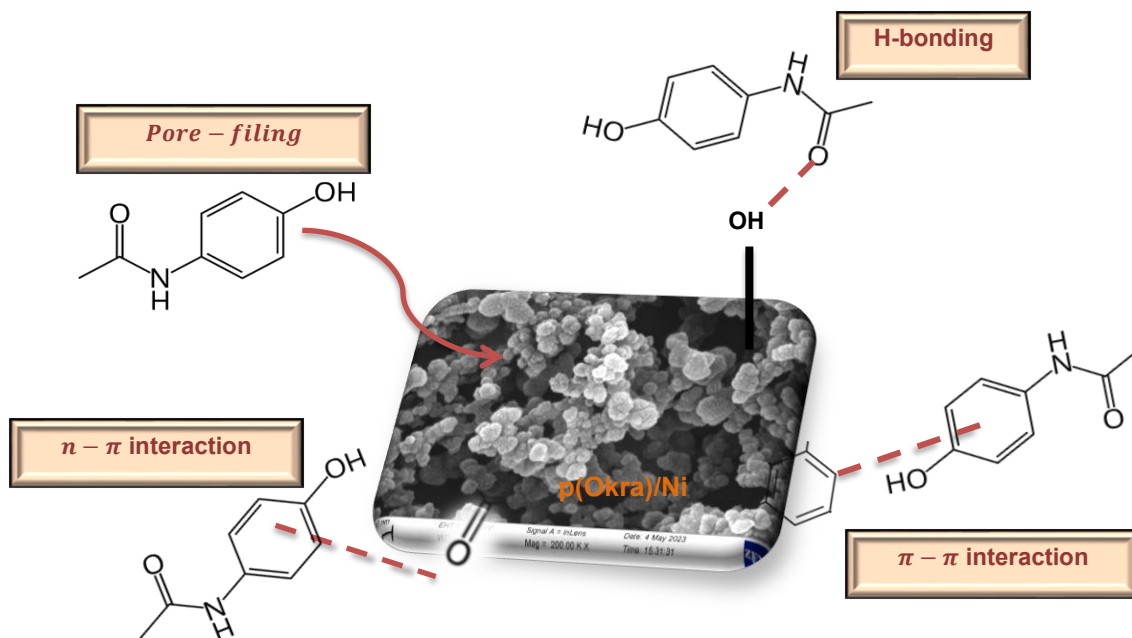


Figure 7. Mechanism of sorption for acetaminophen by p(Okra)/Ni particle (adapted from Ref. [28], with permission from Elsevier).

Conclusions

In this study, p(Okra)/Ni-based polymeric particles synthesized from agricultural okra waste were successfully developed and evaluated for the removal of acetaminophen, a common pharmaceutical contaminant. Comprehensive characterization using SEM, TGA, FT-IR, BET, zeta potential, and particle size analysis confirmed the successful incorporation of Ni ions into the polymer matrix. The BET surface areas of p(Okra), p(Okra)/Ni₁, and p(Okra)/Ni₁₀ were determined to be 86.89 m²/g, 88.38 m²/g, and 83.71 m²/g, respectively. TGA analysis revealed a five-step degradation pattern in p(Okra)/Ni₁₀, with the major thermal decomposition occurring between 295°C and 447°C, resulting in a total mass loss exceeding 83%. Among the synthesized sorbents, p(Okra)/Ni₁ exhibited the highest acetaminophen sorption capacity, reaching 592.1 mg/g at a dosage of 0.0025 g. pH-dependent sorption behavior demonstrated optimal uptake at pH 7, with sorption capacities of 331.3 mg/g for p(Okra)/Ni₁ and 308.9 mg/g for p(Okra)/Ni₃. Temperature-dependent studies indicated enhanced sorption up to 30°C, with maximum capacities of 280.7 mg/g (p(Okra)/Ni₁) and 263 mg/g (p(Okra)/Ni₃) observed at pH 9. Sorption isotherm modeling showed that the Langmuir model provided the best fit to the experimental data, with correlation coefficients (R^2) > 0.99 for both materials. The theoretical maximum sorption capacities were consistent with experimental results, calculated as 500 mg/g for p(Okra)/Ni₁ and 454.6 mg/g for p(Okra)/Ni₃. Thermodynamic analysis indicated negative ΔH° values, confirming the exothermic nature of the sorption process, while positive ΔG° values suggested that sorption is non-spontaneous under the tested conditions. Compared to other sorbents reported in the literature, the p(Okra)/Ni-based particles demonstrated competitive sorption performance. Their surface rich in polar functional groups supported multiple sorption mechanisms, including π - π interactions, n - π electron donor-acceptor interactions, hydrogen bonding, and pore filling, all of which contributed to the high affinity for acetaminophen. The well-developed mesoporous structure of the particles further enhanced mass transfer and drug entrapment. In conclusion, the results confirm that p(Okra)/Ni particles derived from agricultural waste are not only highly efficient in removing acetaminophen from aqueous solutions but also represent a sustainable, low-cost, and environmentally friendly solution for the treatment of pharmaceutical-laden wastewater. Going forward, the design of biosorbents should focus on balancing sorption performance with economic feasibility and environmental compatibility, ensuring scalable and practical applications in sustainable water treatment technologies.

Despite the promising findings of this study, several limitations should be acknowledged. The sorption experiments were conducted under controlled laboratory conditions using synthetic aqueous acetaminophen solutions, which may not fully represent the complexity of real wastewater systems. The effects of competing contaminants, natural organic matter, and varying water chemistries were not investigated. In addition, sorbent regeneration, reusability, long-term stability, and economic feasibility for large-scale applications were beyond the scope of the present study. Therefore, future studies should focus on evaluating the performance of p(Okra)/Ni sorbents in real wastewater matrices and continuous treatment systems to further assess their practical applicability.

Conflicts of Interest

The authors declare that there is no conflict of interest regarding the publication of this paper.

References

- [1] Luo, Y. L., Guo, W. S., Ngo, H. H., Nghiem, L. D., Hai, F. I., Zhang, J., Liang, S., & Wang, X. C. C. (2014). A review on the occurrence of micropollutants in the aquatic environment and their fate and removal during wastewater treatment. *Science of the Total Environment*, 473, 619-641. <https://doi.org/10.1016/j.scitotenv.2013.12.065>
- [2] Fent, K., Weston, A. A., & Caminada, D. (2006). Ecotoxicology of human pharmaceuticals. *Aquatic Toxicology*, 76, 122-159. <https://doi.org/10.1016/j.aquatox.2005.09.009>
- [3] Bolong, N., Ismail, A. F., Salim, M. R., & Matsuura, T. (2009). A review of the effects of emerging contaminants in wastewater and options for their removal. *Desalination*, 239, 229-246. <https://doi.org/10.1016/j.desal.2008.03.020>
- [4] Lapworth, D. J., Baran, N., Stuart, M. E., & Ward, R. S. (2012). Emerging organic contaminants in groundwater: A review of sources, fate and occurrence. *Environmental Pollution*, 163, 287-303. <https://doi.org/10.1016/j.envpol.2011.12.034>
- [5] Vergara-Araya, M., Oeltze, H., Radeva, J., Roth, A. G., Gobbert, C., Niestroj-Pahl, R., Dahne, L., & Wiese, J. (2022). Operation of hybrid membranes for the removal of pharmaceuticals and pollutants from water and wastewater. *Membranes*, 12(5), 502. <https://doi.org/10.3390/membranes12050502>
- [6] Thomas, P. M., & Foster, G. D. (2005). Tracking acidic pharmaceuticals, caffeine, and triclosan through the wastewater treatment process. *Environmental Toxicology and Chemistry*, 24, 25-30. DOI: 10.1897/04-144r.1
- [7] Barbosa, M. O., Moreira, N. F. F., Ribeiro, A. R., Pereira, M. F. R., & Silva, A. M. T. (2016). Occurrence and removal of organic micropollutants: An overview of the watch list of EU Decision 2015/495. *Water Research*, 94, 257-279. <https://doi.org/10.1016/j.watres.2016.02.047>
- [8] Mompelat, S., Le Bot, B., & Thomas, O. (2009). Occurrence and fate of pharmaceutical products and by-

- products, from resource to drinking water. *Environment International*, 35, 803-814. DOI: 10.1016/j.envint.2008.10.008
- [9] Runjavec, M. S., Domanovac, M. V., & Mestrovic, E. (2022). Removal of organic pollutants from real pharmaceutical industrial wastewater with environmentally friendly processes. *Chemical Papers*, 76, 1423-1431. <https://doi.org/10.1007/s11696-021-01919-x>
- [10] Popaliya, M., & Mishra, A. (2023). Modified zeolite as an adsorbent for dyes, drugs, and heavy metal removal: a review. *International Journal of Environmental Science and Technology*, 20, 12919–12936. <https://doi.org/10.1007/s13762-022-04603-z>
- [11] Marques, S. C. R., Marcuzzo, J. M., Baldan, M. R., Mestre, A. S., & Carvalho, A. P. (2017). Pharmaceuticals removal by activated carbons: Role of morphology on cyclic thermal regeneration. *Chemical Engineering Journal*, 321, 233-244. <https://doi.org/10.1016/j.cej.2017.03.101>
- [12] Spessato, L., Bedin, K. C., Cazetta, A. L., Souza, I., Duarte, V. A., Crespo, L. H. S., Silva, M. C., Pontes, R. M., & Almeida, V. C. (2019). KOH-super activated carbon from biomass waste: Insights into the paracetamol adsorption mechanism and thermal regeneration cycles. *Journal of Hazardous Materials*, 371, 499-505. <https://doi.org/10.1016/j.jhazmat.2019.02.102>
- [13] Khan, A. H., Khan, N. A., Zubair, M., Shaida, M. A., Manzar, M. S., Abutaleb, A., Naushad, M., & Iqbal, J. (2022). Sustainable green nano-adsorbents for remediation of pharmaceuticals from water and wastewater: A critical review. *Environmental Research*, 204, 112243.
- [14] Yildiz H, Gülşen H, Şahin Ö, Baytar O, & Kutluay S. Novel adsorbent for malachite green from okra stalks waste: synthesis, kinetics and equilibrium studies. *International Journal of Phytoremediation*, 2024; 26(3), 369-381.
- [15] Calisto, V., Jaria, G., Silva, C. P., Ferreira, C. I. A., Otero, M., & Esteves, V. I. (2017). Single and multi-component adsorption of psychiatric pharmaceuticals onto alternative and commercial carbons. *Journal of Environmental Management*, 192, 15-24. <https://doi.org/10.1016/j.jenvman.2017.01.029>
- [16] Ouyang, J. B., Zhou, L. M., Liu, Z. R., Heng, J. Y. Y., & Chen, W. Q. (2020). Biomass-derived activated carbons for the removal of pharmaceutical micropollutants from wastewater: A review. *Separation and Purification Technology*, 253, 117536. <https://doi.org/10.1016/j.seppur.2020.117536>
- [17] Wang, F., Qi, X., Zhang, H., & Yang, Z. (2025). Innovative molten salt techniques for biomass valorization: transforming biomass into advanced carbon materials. *Carbon*, 234, 119999. <https://doi.org/10.1016/j.carbon.2025.119999>
- [18] Oussadi, K., Al-Farraj, S., Benabdallah, B., Benettayeb, A., Haddou, B., & Sillanpaa, M. (2025). Wool keratin as a novel, alternative, low-cost adsorbent rich in various –N and –S proteins for eliminating methylene blue from water. *Biomass Conversion and Biorefinery*, 15, 4803–4817. <https://doi.org/10.1007/s13399-024-05851-4>.
- [19] Amar, I. A., Abdulqadir, M. A., Benettayeb, A., Lal, B., Shamsi, S. A., & Hosseini-Bandegharai, A. (2024). Cerium-doped calcium ferrite for malachite green dye removal and antibacterial activities. *Chemistry Africa*, 7, 1423–1441. <https://doi.org/10.1007/s42250-023-00834-w>.
- [20] Sun, L., Jiang, Z., Yuan, B., Zhi, S., Zhang, Y., Li, J., & Wu, A. (2021). Ultralight and superhydrophobic perfluorooctyltrimethoxysilane modified biomass carbonaceous aerogel for oil-spill remediation. *Chemical Engineering Research and Design*, 174, 71-78. <https://doi.org/10.1016/j.cherd.2021.08.002>
- [21] Zhu, X. M., Xu, R., Wang, H., Chen, J. Y., & Tu, Z. C. (2020). Structural properties, bioactivities, and applications of polysaccharides from Okra [*Abelmoschus esculentus* (L.) Moench] : A Review. *Journal of Agricultural and Food Chemistry*, 68, 14091-14103. DOI: 10.1021/acs.jafc.0c04475
- [22] Hazarika, A., Hazarika, I., Gogoi, M., Bora, S. S., Borah, R. R., Goutam, P. J., & Saikia, N. (2018). Use of a plant based polymeric material as a low cost chemical admixture in cement mortar and concrete preparations. *Journal of Building Engineering*, 15, 194-202. <https://doi.org/10.1016/j.jobe.2017.11.017>
- [23] Ghorri, M. U., Alba, K., Smith, A. M., Conway, B. R., & Kontogiorgos, V. (2014). Okra extracts in pharmaceutical and food applications. *Food Hydrocolloids*, 42, 342-347. <https://doi.org/10.1016/j.foodhyd.2014.04.024>
- [24] Araujo, A., Galvao, A., Silva, C., Mendes, F., Oliveira, M., Barbosa, F., Sousa, M., & Bastos, M. (2018). Okra mucilage and corn starch bio-based film to be applied in food. *Polymer Testing*, 71, 352-361. <https://doi.org/10.1016/j.polymertesting.2018.09.010>
- [25] Zhang, T., Xiang, J. L., Zheng, G. B., Yan, R. Q., & Min, X. (2018). Preliminary characterization and anti-hyperglycemic activity of a pectic polysaccharide from okra (*Abelmoschus esculentus* (L.) Moench). *Journal of Functional Foods*, 41, 19-24. <https://doi.org/10.1016/j.jff.2017.12.028>
- [26] Gao, H., Zhang, W. C., Wu, Z. Y., Wang, H. Y., Hui, A. L., Meng, L., Chen, P. P., Xian, Z. J., He, Y. W., Li, H. H., Du, B., & Zhang, H. W. (2018). Preparation, characterization and improvement in intestinal function of polysaccharide fractions from okra. *Journal of Functional Foods*, 50, 147-157. <https://doi.org/10.1016/j.jff.2018.09.035>
- [27] Ghumman, S. A., Bashir, S., Noreen, S., Khan, A. M., Riffat, S., & Abbas, M. (2018). Polymeric microspheres of okra mucilage and alginate for the controlled release of oxcarbazepine: In vitro & in vivo evaluation. *International Journal of Biological Macromolecules*, 111, 1156-1165. <https://doi.org/10.1016/j.ijbiomac.2018.01.058>
- [28] Ersen Dudu, T., Alpaslan, D., Saliyeva, K., & Borkoyev, B. (2025). Highly efficient removal of paracetamol from wastewater using novel crosslinked okra-based metal composite sorbents. *Materials Today Communications*, 45, 112313. <https://doi.org/10.1016/j.mtcomm.2025.112313>
- [29] Murtaza, F., Akhter, N., Qamar, M. A., Yaqoob, A., Chaudhary, A. A., Patil, B. R., Khan, S. U.-D., Ibrahim, N. A., Basher, N. S., Aleissa, M. S., Kanwal, I., & Imran, M. (2024). *Syzygium aromaticum* bud extracted core-shell Ag-Fe bimetallic nanoparticles: phytotoxic, antioxidant, insecticidal, and antibacterial properties. *Crystals*, 14(6), 510. <https://doi.org/10.3390/cryst14060510>
- [30] Alpaslan, D., & Ersen Dudu, T. (2021). Removal of As(V), Cr(VI) and Cr(III) heavy metal ions from environmental waters using amidoxime and quaternized hydrogels. *Manas Journal of Engineering*, 9(2), 104-

114. <https://doi.org/10.51354/mjen.936970>
- [31] Langmuir, I. (1918). The adsorption of gases on plane surfaces of glass, mica and platinum. *Journal of the American Chemical Society*, 40, 1361-1403. <http://dx.doi.org/10.1021/ja02242a004>
- [32] Freundlich, H. M. F. (1906). Über die adsorption in losungen. *Zeitschrift für Physikalische Chemie*, 57, 385-470.
- [33] Tempkin, M. I., & Pyzhev, V. (1940). Kinetics of ammonia synthesis on promoted iron catalyst. *Acta Physicochim URSS*, 12, 327-356.
- [34] Dubinin, M. M. (1960). The potential theory of adsorption of gases and vapors for adsorbents with energetically non-uniform surface. *Chemical Reviews*, 60, 235-241. <https://doi.org/10.1021/cr60204a006>
- [35] Gibbs, J. W. (1928). *The collected works of J. Willard Gibbs*. New York : Longmans, Green and Co.
- [36] Tasar, S., & Ozer, A. (2020). A Thermodynamic and kinetic evaluation of the adsorption of Pb(II) ions using peanut (*arachis hypogaea*) shell-based biochar from aqueous media. *Polish Journal of Environmental Studies*, 29, 293-305. <https://doi.org/10.15244/pjoes/103027>
- [37] Mohanty, A. K., Misra, M., & Hinrichsen, G. (2000). Biofibres, biodegradable polymers and biocomposites: an overview. *Macromolecular Materials and Engineering*, 276/277, 1–24. [https://doi.org/10.1002/\(SICI\)1439-2054\(20000301\)276:1<1::AID-MAME1>3.0.CO;2-W](https://doi.org/10.1002/(SICI)1439-2054(20000301)276:1<1::AID-MAME1>3.0.CO;2-W)
- [38] Wang, Z., Wu, J., Shi, X., Song, F., Gao, W., & Liu, S. (2020). Stereocomplexation of poly(lactic acid) and chemical crosslinking of Ethylene Glycol Dimethacrylate (EGDMA) double-crosslinked temperature/pH dual responsive hydrogels. *Polymers*, 12(10), 2204. <https://doi.org/10.3390/polym12102204>
- [39] Blindheim, F. H., & Ruwoldt, J. (2025). Quantifying the abundance of alkane moieties in lignins with ftir spectroscopy and pls regression; estimating grafting degree of esterification. *ChemSusChem*, 18(3), e202400938. <https://doi.org/10.1002/cssc.202400938>
- [40] Abdullah, N., Mahmud, R. A., Jusoh, R., Beg, M. D. H., & Islam, M. R. (2021). Effects of chemical modification on the performance evaluation of photoinitiated, dispersion-polymerized poly(Methyl Methacrylate-co-Ethylene Glycol Dimethacrylate-co-Vinylbenzyl Chloride) microsphere. *Polymers and Polymer Composites*, 29(5), 362–372. <https://doi.org/10.1177/096739112091786>
- [41] Rosas-Reyes, R., Reyes-Ortega, Y., Morales-Juarez, T. J., Gómez-Vidales, V., & García-Orozco, I. (2017). Synthesis of a one-dimensional coordination polymer of Nickel(II) complex with a β -Oxodithioester ligand. *Journal of Chemistry*, 2017(11), 1-7. <https://doi.org/10.1155/2017/7623210>
- [42] Danilova, J. S., Avdoshenko, S. M., Karushev, M. P., Timonov, A. M., & Dmitrieva, E. (2021). Infrared spectroscopic study of nickel complexes with salen-type ligands and their polymers. *Journal of Molecular Structure*, 1241, 130668. <https://doi.org/10.1016/j.molstruc.2021.130668>
- [43] Zhao, Y., Yang, S., Wang, G., & Han, M. (2015). Adsorption behaviors of acetaminophen onto the colloid in sediment. *Polish Journal of Environmental Studies*, 24(2), 853-861. DOI: 10.15244/pjoes/31338
- [44] Juela, D. M. (2020). Comparison of the adsorption capacity of acetaminophen on sugarcane bagasse and corn cob by dynamic simulation. *Sustainable Environment Research*, 30(1), 1-13. <https://doi.org/10.1186/s42834-020-00063-7>
- [45] Deng, H., Lu, J., Li, G., Zhang, G., & Wang, X. (2011). Adsorption of methylene blue on adsorbent materials produced from cotton stalk. *Chemical Engineering Journal*, 172(1), 326-334. <https://doi.org/10.1016/j.cej.2011.06.013>
- [46] Obradovic, M., Dakovic, A., Smiljanic, D., Ozegovic, M., Marković, M., Rottinghaus, G. E., & Krstic, J. (2022). Ibuprofen and diclofenac sodium adsorption onto functionalized minerals: Equilibrium, kinetic and thermodynamic studies. *Microporous and Mesoporous Materials*, 335, 111795. <https://doi.org/10.1016/j.micromeso.2022.111795>
- [47] Bakyt, B., Ersen Dudu, T., Kalipa, S., & Alpaslan, D. (2024). The efficiency of cationic-based hydrogels in heavy metal removal from wastewater. *Polymer Bulletin*, 81, 7273–7293. DOI: 10.1007/s00289-023-05066-z
- [48] Ersen Dudu, T., Alpaslan, D., & Aktas, N. (2022). Synthesis of controlled release hydrogels from dimethylacrylamide/ maleic acid/starch and its application in lettuce cultivation. *Journal of Polymer Research*, 29, 524. DOI: 10.1007/s10965-022-03363-1
- [49] Reddad, Z., Gerente, C., Andres, Y., & Le, Cloirec, P. (2002). Adsorption of several metal ions onto a low-cost biosorbent: kinetic and equilibrium studies. *Environmental Science & Technology*, 36, 2067-2073. <https://doi.org/10.1021/es0102989>
- [50] Sarkar, M., Sarkar, A. R., & Goswami, J. L. (2007). Mathematical modeling for the evaluation of zinc removal efficiency on clay sorbent. *Journal of Hazardous Materials*, 149, 666-674. <https://doi.org/10.1016/j.jhazmat.2007.04.027>
- [51] Patel, M., Kumar, R., Pittman, C. U., & Mohan, D. (2021). Ciprofloxacin and acetaminophen sorption onto banana peel biochars: environmental and process parameter influences. *Environmental Research*, 201, 111218. <https://doi.org/10.1016/j.envres.2021.111218>
- [52] Spessato, L., Cazetta, A. L., Melo, S., Pezoti, O., Tami, J., Ronix, A., Fonseca, J. M., Martins, A. F., Silva, T. L., & Almeida, V. C. (2020). Synthesis of superparamagnetic activated carbon for paracetamol removal from aqueous solution. *Journal of Molecular Liquids*, 300, 112282. <https://doi.org/10.1016/j.molliq.2019.112282>
- [53] Kerkhoff, C. M., da Boit Martinello, K., Franco, D. S. P., Netto, M. S., Georgin, J., Foletto, E. L., Piccilli, D. G. A., Silva, L. F. O., & Dotto, G. L. (2021). Adsorption of ketoprofen and paracetamol and treatment of a synthetic mixture by novel porous carbon derived from *Butia capitata* endocarp. *Journal of Molecular Liquids*, 339, 117184.
- [54] Parus, A., Gaj, M., Karbowska, B., & Zembrzusk, J. (2020). Investigation of acetaminophen adsorption with a biosorbent as a purification method of aqueous solution. *Chemistry and Ecology*, 36(7), 705–725. <https://doi.org/10.1080/02757540.2020.1757081>
- [55] Njoku, C. B., & Msagati, T. A. M. (2022). Adsorption technique for the removal of acetaminophen as adsorbate contaminant from water with metals and eggshell. *Desalination and Water Treatment*, 249, 87–102.

- <https://doi.org/10.5004/dwt.2022.28086>
- [56] Yanan, C., Srour, Z., Ali, J., Guo, S., Taamalli, S., Fevre-Nollet, V., da Boit Martinello, K., Georjgin, J., Franco, D. S. P., Silva, L. F. O., Dotto, G. L., Erto, A., Louis, F., El Bakali, A., & Sellaoui, L. (2023). Adsorption of paracetamol and ketoprofenon activated charcoal prepared from the residue of the fruit of Butiacapitate: experiments and theoretical interpretations. *Chemical Engineering Journal*, 454, 139943. <https://doi.org/10.1016/j.cej.2022.139943>
- [57] Akpotu, S. O., & Moodley, B. (2018). Application of as-synthesized MCM41 and MCM-41 wrapped with reduced graphene oxide/ graphene oxide in the remediation of acetaminophen and aspirin from aqueous system. *Journal of Environmental Management*, 209, 205–215. <https://doi.org/10.1016/j.jenvman.2017.12.037>
- [58] Aminul Islam, Md., Nazal, M. K., Akinpelu, A. A., Sajid, M., Alhussain, N. A., & Ilyas, M. (2024). High performance adsorptive removal of emerging contaminant paracetamol using a sustainable biobased mesoporous activated carbon prepared from palm leaves waste. *Journal of Analytical and Applied Pyrolysis*, 180, 106546. <https://doi.org/10.1016/j.jaap.2024.106546>
- [59] Igwegbe, C. A., Aniagor, C. O., Oba, S. N., Yap, P. S., Iwuchukwu, F. U., Liu, T., de Souza, E. C., & Ighalo, J. O. (2021). Environmental protection by the adsorptive elimination of acetaminophen from water: a comprehensive review. *Journal of Industrial and Engineering Chemistry*, 104, 117–135. <https://doi.org/10.1016/j.jiec.2021.08.015>
- [60] dos Reis, G. S., Guy, M., Mathieu, M., Jebrane, M., Lima, E. C., Thyrel, M., Dotto, G. L., & Larsson, S. H. (2022). A comparative study of chemical treatment by $MgCl_2$, $ZnSO_4$, $ZnCl_2$, and KOH on physicochemical properties and acetaminophen adsorption performance of biobased porous materials from tree bark residues. *Colloids and Surfaces A: Physicochemical and Engineering Aspects*, 642, 128626. <https://doi.org/10.1016/j.colsurfa.2022.128626>